Local control of microdomain orientation in diblock copolymer thin films with...
Morkved, T L; Lu, M; Urbas, A M; Ehrichs, E E; et al
Science; Aug 16, 1996; 273, 5277; Research Library
pg. 931

■ REPORTS

Local Control of Microdomain Orientation in Diblock Copolymer Thin Films with Electric Fields

T. L. Morkved, M. Lu, A. M. Urbas, E. E. Ehrichs,* H. M. Jaeger,† P. Mansky, T. P. Russell

Local control of the domain orientation in diblock copolymer thin films can be obtained by the application of electric fields on micrometer-length scales. Thin films of an asymmetric polystyrene-polymethylmethacrylate diblock copolymer, with cylindrical polymethylmethacrylate microdomains, were spin-coated onto substrates previously patterned with planar electrodes. The substrates, 100-nanometer-thick silicon nitride membranes, allow direct observation of the electrodes and the copolymer domain structure by transmission electron microscopy. The cylinders aligned parallel to the electric field lines for fields exceeding 30 kilovolts per centimeter, after annealing at 250°C in an inert atmosphere for 24 hours. This technique could find application in nanostructure fabrication.

A number of strategies for nanostructure fabrication are currently being developed on the basis of self-assembly (1). One approach is to take advantage of the pattern formation of block copolymers, which are composed of two different polymer chains covalently bonded together on one end. Polymers are usually immiscible with one another and phase-separate; in block copolymers, molecular connectivity forces phase separation to occur on molecular-length scales. As a result, periodically ordered nanometer-sized microdomains (such as lamellae, cylinders, or spheres) form (2), and their specific chemical, electrical, optical, or mechanical properties can be controlled by the choice of the constituent polymers (3–5). Thin films can be formed by spin coating and, after thermal annealing, display well-ordered microdomain patterns (5–7). By removing one polymer chemically, these patterns may be transferred to a substrate through etching or evaporation (5), or the domains can serve as a template for decoration with nanoparticles (3).

A significant limitation of these techniques is a lack of control over the orientation of the microdomains. In bulk samples, uniform alignment of the microdomains can be achieved by the application of shear to a copolymer melt (8), but this technique cannot be applied easily (if at all) to thin films. Amundson et al. showed (9, 10) that the lamellar microdomains of a block copolymer melt of polystyrene (PS) and poly-

T. L. Morkved, M. Lu, A. M. Urbas, E. E. Ehrichs, H. M. Jaeger, James Franck Institute and Department of Physics, University of Chicago, Chicago, IL 60637, USA.
P. Mansky and T. P. Russell, IBM Research Division, Almaden Research Center, 650 Harry Road, San Jose, CA 95120, USA.

*Present address: Advanced Micro Devices, 5204 East Ben White Boulevard, Austin, TX 78741, USA.
†To whom correspondence should be addressed.

methylmethacrylate (PMMA), denoted P(S-b-MMA), could be induced to align parallel to a strong applied electric field and proposed that the field was coupled to the spatial variation of the dielectric constant, ε, limited by the dynamics of defect motion. Although they pointed out the possibility of inducing locally anisotropic material properties, they found electric fields (E fields) to be inferior to shear for aligning bulk samples (11). The high voltages required (1 kV or more for millimeter and larger sized samples) also are a disadvantage.

We show that E fields are, in fact, ideally suited to the local control of the domain orientation in block copolymer thin films. The high E fields needed can be achieved with potentials of only a few volts for electrodes separated by several micrometers. Although we used a simple electrode configuration in our studies, the results show that the cylinders can follow both straight and curved E field lines. Thus, not only can the alignment direction be independently specified at various locations in a film if multiple sets of electrodes are used, but also a spatially varying cylinder orientation can be imposed if the electrode geometry is tailored.

An asymmetric P(S-b-MMA) diblock copolymer was used with a PS volume fraction of 0.66, an average molecular weight of 1.01×10^5, and a polydispersity of 1.09. We prepared thin films by spin-casting a 2% solution of the copolymer in toluene onto amorphous silicon nitride substrates with prefabricated electrodes separated by 4 μm (Fig. 1) (12). Cylindrical microdomains of PMMA in a PS matrix form in these films when annealed above the glass temperature. Under an applied, in-plane E field, the films were then annealed in an argon atmosphere at 250°C for 24 hours (13) and cooled at a rate of 0.5°C/min to room tem-

perature. Finally, the resulting film morphology was examined in a Phillips CM120 transmission electron microscope (TEM) operated at 120 kV.

The silicon nitride substrates are TEM-transparent and mechanically robust, and thus electrode fabrication, sample processing, and TEM imaging do not require removal of the film from the substrate (14). Earlier TEM studies of block copolymer thin films have involved either stripping a film from a substrate for imaging or casting a film directly on a C-coated TEM mesh (7, 15). The film thickness was chosen such that the films consisted of a single layer of cylindrical microdomains lying parallel to the substrate. The cylinders are easily detected by TEM (white lines in Fig. 2). The contrast arises from the radiation-induced thinning of the PMMA (16). Slightly thicker films, not shown, produced mixed structures of cylinders both parallel and perpendicular to the substrate (7), which shows that the PMMA microdomains are indeed cylinders and not lamellae oriented normal to the substrate.

When a film is annealed without an E field present, the cylinder orientation is random (Fig. 2C). Such films contain a large number of defects as well as highly curved cylindrical domains. The orientation of the cylinders is not influenced by the presence of the electrodes. The electrode thickness was kept small (25 nm) to reduce the likelihood of preferential cylinder orientation at the electrode edges. Markedly different results were obtained in the central gap region after annealing in an E field of 37 kV/cm (corresponding to an applied potential difference of 15 V). In this instance, the cylinders are essentially parallel to each other and to the field in the central gap region, with few defects, and the cylinder separation of 60 nm is near that observed in the absence of the E field (Fig. 2B). The cylinders also follow the curvature of the field lines outside the central gap
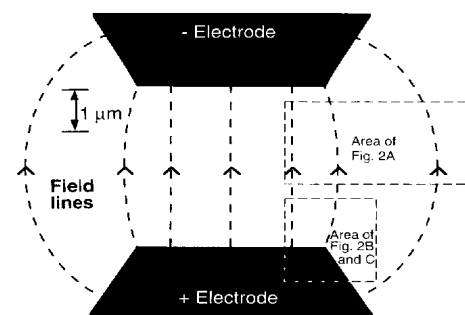

Fig. 1. Sketch of a top view of a typical electrode layout, along with the corresponding E field lines. The areas defined by the boxes outline the fields of view for the micrographs shown in Fig. 2, A to C.

region. There is a gradual transition from highly aligned (left) to unaligned behavior (right) with decreasing electric field strength (Fig. 2A) (compare with Fig. 1).

The E field at any position within the film can be calculated for the actual electrode configuration, if we assume a two-dimensional (2D) geometry. By analyzing digitized TEM micrographs as in Fig. 2, we found that the local field strength and direction can be correlated with the observed orientation of the cylinders. We can quantify the degree of alignment as a function of field strength, E. For each cylinder segment, we define θ as the included angle between the direction of the cylinder axis, $\hat{e}_c$, and the direction of the electric field, $\hat{e}_z$. A suitable 2D orientational order parameter can be written as $S(E) \propto (2 < \cos^2\theta > -1)$, where we average over all regions with local field strength E within the analyzed field of view. When averaged over a sufficiently large area, $S(E)$ will be zero in a macroscopically unaligned sample. For ideal alignment, $S(E)$ approaches unity and $\hat{e}_c$ is parallel to $\hat{e}_z$ everywhere (17).

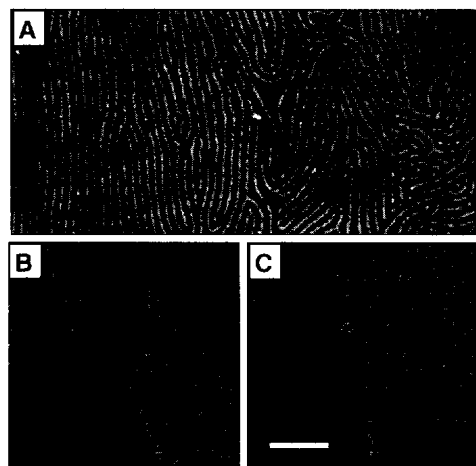Figure 3 shows S as a function of E^2 for

Fig. 2. TEM micrographs of cylindrical-phase, diblock copolymer films in the region between the electrodes (see boxes in Fig. 1). The lighter lines are cylinders of PMMA surrounded by a darker PS background. At this film thickness, a single layer of cylinders results, lying in a plane parallel to the substrate. The cylinder repeat spacing is 60 nm. All three samples were prepared under identical annealing conditions. The scale is the same for all three micrographs (bar, 500 nm). (**A**) Close-up of a region halfway between electrodes, indicating a gradual transition from well-aligned cylinders (left edge, $E \approx 37$ kV/cm) near the central electrode gap to random cylinder orientations (right edge, $E \approx 20$ kV/cm) as the E field strength drops off outside the central gap. (**B** and **C**) Close-ups of regions near a corner of one electrode: annealed in the presence of an applied E field (B) and without field (C). The cylinders follow the curved E-field lines in (B) near the electrode edge.

the sample in Fig. 2, A and B; E^2 is a measure of the energy contributed by the electric field (see below). As seen from Fig. 3, $S(E)$ is large and, within the accuracy of our analysis, field-independent above ~ 30 kV/cm, but decreases rapidly as E falls below this value. The crossover marks the change from nearly complete to partial alignment outside the central electrode gap region, where E drops off. The saturation at $\sim 80\%$ is caused by residual point defects, disclination lines, and wall defects. The E required for strong orientation appears to be sample-independent. In different samples, prepared with varying gap widths or applied voltages, a high degree of alignment was never observed for $E < 30$ kV/cm, even in the central gap.

In an E field, a system of two dielectrics has its lowest energy when the interface is oriented parallel to the field. This configurational energy, due to the difference in dielectric constants, $\Delta\varepsilon$, can be calculated from electrostatics. Amundson et al. (9, 10) used this approach to build a theory for the weak segregation limit of diblock copolymers. They found that, indeed, the lowest energy state exhibits microdomains parallel to the electric field (18). Although their analysis treated bulk copolymers, we can use it as a starting point to interpret our results. In the strong segregation limit (that is, highly segregated domains), we can estimate the reduction in electrostatic energy associated with the alignment of the copolymer studied here. Consider two domain orientations containing cylinders either all parallel or all perpendicular to the applied E field. The free energy difference per unit volume, ΔF, is proportional to $(\Delta\varepsilon E)^2$. For the high-temperature values (19) of $\varepsilon_{PS} = 2.45$ and $\varepsilon_{PMMA} \approx 6$, we obtain $\Delta F \approx 130$ eV/μm^3 at the crossover field of 30 kV/cm (20). For our experiments, the quantity of importance is the energy difference, ΔF^*, between the parallel and random orientations, which corresponds to half the above

Fig. 3. Normalized order parameter S plotted as a function of the square of the electric field strength, E^2.

value (65 eV/μm^3).

For a spun-cast sample annealed without field, a highly curved domain morphology results (as in Fig. 2C) with a high density of defects and only short-range ordering of the cylinders. Collective motion leading to improved ordering is limited by the associated energy barriers, which may be greater than those in the bulk as a result of pinning arising from the substrate or the reduced dimensionality (5). If these energy barriers are the same ones that must be overcome by the E field to produce an aligned state, then the energy due to defects and cylinder curvature in a morphology such as in Fig. 2C should be comparable to the threshold energy, ΔF^*, for field-induced alignment. We can estimate the curvature energy in such a configuration from $\Delta F_{curv} = K_1/(2L^2)$, where L is the average value for the bending radius of curvature of the cylinders and K_1 is the splay elastic coefficient ($\approx 10^{-7}$ dyne for our polymer) (21). By analyzing images like Fig. 2C, we can estimate that the radius of curvature lies in the range of 100 to 500 nm with an average L of ~ 200 nm. This analysis yields an estimate of ~ 80 eV/μm^3 for ΔF_{curv}. The remarkably close agreement of this value with the threshold energy, $\Delta F^* \approx 65$ eV/μm^3, must be considered fortuitous, given the rough nature of these estimates, and it is only the similar magnitude of these energy scales that is important (22). Nevertheless, this agreement clearly demonstrates that body forces, induced by applied electric fields, provide a viable mechanism for the alignment of copolymer domains.

Our technique could find application in fabricating nanostructures. First, scaling up can be achieved through the use of interdigitated electrodes with local gaps of the order of 10 μm. Tailoring of various cylinder orientations should be possible over areas of many square centimeters. Second, the planar electrodes used to control the orientation of the polymer patterns may subsequently serve as direct electrical contacts to the resulting structures. If liquid crystal–type copolymers are used, electro-optically active devices may be realized. If the cylinder domains can be made conducting, for example, through selective metal decoration (3), the self-assembly of parallel quantum wires between the electrodes becomes feasible. In this way, our technique allows for the direct integration of self-assembly with ordinary microlithographic techniques.

REFERENCES AND NOTES

1. G. M. Whitesides, J. P. Mathias, C. T. Seto, Science 254, 1312 (1991).
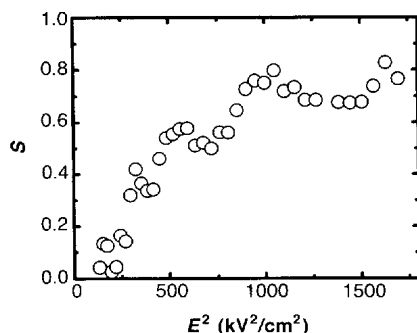2. F. S. Bates and G. H. Fredrickson, Annu. Rev. Phys. Chem. 41, 525 (1990).

3. T. L. Morkved, P. Wiltzius, H. M. Jaeger, D. G. Grier, T. A. Witten, *Appl. Phys. Lett.* **64**, 422 (1994); R. Saito, S. Okamura, K. Ishizu, *Polymer* **33**, 1099 (1992); K. Ishizu et al., *ibid.* **34**, 2256 (1993); R. S. Saunders, R. E. Cohen, R. R. Schrock, *Macromolecules* **24**, 5599 (1991); Y. Ng, C. Chan, R. R. Schrock, R. E. Cohen. *Chem. Mater.* **4**, 24 (1992); R. Tassoni and R. R. Schrock, *ibid.* **6**, 744 (1994).
4. J. P. Spatz, A. Roescher, S. Sheiko, G. Krausch, M. Moller, *Adv. Mater.* **7**, 731 (1995).
5. P. Mansky, P. Chaikin, E. L. Thomas, *J. Mater. Sci.* **30**, 1987 (1995); *Appl. Phys. Lett.* **68**, 2586 (1996).
6. E. L. Thomas, D. J. Kinning, D. B. Alward, C. S. Henkee, *Macromolecules* **20**, 2934 (1987).
7. Y. Liu et al., *ibid.* **27**, 4000 (1994).
8. A. Keller, E. Pedemonte, F. M. Willmouth, *Nature* **225**, 538 (1970); G. Hadziiannou, A. Mathis, A. Skoulious, *Colloid Polym. Sci.* **257**, 136 (1979); K. A. Koppi, M. Tirrell, F. S. Bates, K. Almdal, R. H. Colby, *J. Phys. (Paris)* **2**, 1941 (1993).
9. K. Amundson et al., *Macromolecules* **24**, 6546 (1991); K. Amundson, E. Helfand, X. Quan, S. D. Hudson, S. D. Smith, *ibid.* **27**, 6559 (1994).
10. K. Amundson, E. Helfand, X. Quan, S. D. Smith, *ibid.* **26**, 2698 (1993).
11. For related work on polymer blends, see G. Venugopal, S. Krause, G. Wnek, *Chem. Mater.* **4**, 1334 (1992); J. M. Serpico et al., *Macromolecules* **25**, 6373 (1992).
12. Our substrates consisted of a 100-nm-thick silicon nitride layer deposited onto a silicon wafer. The silicon was selectively etched away from the backside of the wafer under small rectangular areas, providing self-supporting, transparent silicon nitride membranes with lateral dimensions of 60 μm. We fabricated planar electrodes with gap spacings of 4 μm on top of the silicon nitride within the window areas using optical or electron-beam lithography followed by evaporation of 25-nm chromium. Small gold wires were attached with silver epoxy and connected to a programmable voltage source.
13. At this temperature, the product of Flory-Huggins interaction parameter, χ, and number of monomers per chain, N, for our polymers is $\chi N \sim 30$, putting us in the strong segregation limit. See T. P. Russell, R. P. Hjelm, P. A. Seeger, *Macromolecules* **23**, 890 (1990); T. P. Russell, *ibid.* **26**, 5819 (1993).
14. T. L. Morkved et al., in preparation.
15. C. S. Henkee, E. L. Thomas, L. J. Fetters, *J. Mater. Sci.* **23**, 1685 (1988).
16. E. L. Thomas and Y. Talmon, *Polymer* **19**, 225 (1978).
17. To minimize systematic errors that arise from the finite resolution of any digital image processing routine, we consider a normalized order parameter S, defined as $S(E) = [C(E) - C_{min}]/(C_{max} - C_{min})$. Here $C(E) = 2 <\cos^2\theta> - 1$; C_{max} and C_{min} are the order parameters obtained by image processing from a perfectly aligned region containing no defects and from an unaligned sample annealed without an applied E field, respectively.
18. E. V. Gurovich [*Macromolecules* **27**, 7063 (1994)] proposed that alignment in polymers is due to field-induced changes in the coil conformations. Because the anisotropic part of the polarizability of most monomers is much smaller than the average polarizability, this mechanism can be neglected for nonpolar systems compared to the effect treated by Amundson et al. [see A. Onuki and J. Fukuda, *Macromolecules* **28**, 8788 (1995)]. Even though PMMA does contain permanent dipoles, we can estimate their contribution and find it not significant [see also the discussion in (*10*)].
19. R. F. Boyer, in *Encyclopedia of Polymer Science and Technology* (Intersciences, New York, 1970), vol. 13, pp. 251–277; N. G. McCrum, B. E. Read, G. Williams, *Anelastic and Dielectric Effects in Polymeric Solids* (Wiley, New York, 1967), p. 264.
20. $\Delta F = (\gamma/8\pi)(\Delta\varepsilon E)^2/\langle\varepsilon\rangle$, in centimeter-gram-second units, where the coefficient γ depends on the details of the domain geometry. In the case of cylindrical domains, as in our samples, $\gamma = 1/9$.
21. K. Amundson and E. Helfand, *Macromolecules* **26**, 1324 (1993).
22. Systematic studies of the effect of changing the annealing conditions are in progress. The degree of alignment in E fields <30 kV/cm might improve with different annealing conditions, leading to a reduction in the saturation field for the order parameter $S(E)$. However, improvements in the ordering of unaligned samples under the same conditions are also likely, leading to an increase in the average radius of curvature and a decrease in the curvature energy.
23. We thank T. A. Witten, F. J. Solis, and S. R. Nagel for helpful discussions. Supported in part by the Medical Research Science and Engineering Center program of the National Science Foundation (NSF) under award DMR-9400379. The silicon nitride membranes were fabricated at the National Nanofabrication Facility at Cornell University, which is supported by the National Science Foundation under grant ECS-8619049. H.M.J. acknowledges fellowship support from the David and Lucile Packard Foundation. T.P.R. and P.M. acknowledge the support of the U.S. Department of Energy, Office of Basic Energy Sciences, under contract FG03-88ER-45375.

12 March 1996; accepted 11 June 1996

Biomembrane Templates for Nanoscale Conduits and Networks

Evan Evans, Howard Bowman, Andrew Leung, David Needham, David Tirrell

Long nanotubes of fluid-lipid bilayers can be used to create templates for photochemical polymerization into solid-phase conduits and networks. Each nanotube is pulled from a micropipette-held feeder vesicle by mechanical retraction of the vesicle after molecular bonding to a rigid substrate. The caliber of the tube is controlled precisely in a range from 20 to 200 nanometers merely by setting the suction pressure in the micropipette. Branched conduits can be formed by coalescing separate nanotubes drawn serially from the feeder vesicle surface. Single nanotubes and nanotube junctions can be linked together between bonding sites on a surface to create a functionalized network. After assembly, the templates can be stabilized by photoinitiated radical cross-linking of macromonomers contained in the aqueous solution confined by the lipid bilayer boundary.

Recent developments in the fabrication of meso- and nanoscale structures have included the self-assembly of carbon and other materials into nanotubes and quantum wires (*1*) and the coalescence of lipid surfactants from solution into submicrometer tubules (*2*). Because of the bulk nature of the processes used to assemble such aggregates, it is difficult to preset the dimensions (such as tube length and the number of layers in the tube wall), and it is even more difficult to pattern macroscopic arrangements of the tube structures. New insights into the mechanics of biomembranes (*3*) led us to develop a simple method for the production of near-millimeter lengths of nanotubes, with calibers set by manual control (to an accuracy of ±10%) in the range of 20 to 200 nm. These tubes can be joined to form branched conduits and complex networks. Because these designs are made possible by the fluid property of the biomembrane interface, the challenge has been to develop chemical strategies to stabilize the membrane templates after patterning. Here, we introduce a method for the layout of nanotube networks and a photochemical polymerization process for stabilization of the resulting patterns in situ.

The formation of bilayer nanotubes from membrane capsules is a common occurrence in cell biology. For example, when a cell or vesicle sticks to a foreign surface at a point and is then pulled away, an optically invisible bilayer tube (diameter <100 nm) usually connects the capsule to the surface even after displacements of many diameters (*4*). Similarly, when vesicles are dehydrated to create large excesses of surface area or when cytoskeletal structures are destroyed inside cells, spherical blebs appear and remain tethered to the outer membrane by invisible bilayer tubes (*5*). The frequent occurrence of tethers shows that the closed spherical topology preferred by lamellar-phase lipids is extremely difficult to disrupt.

Two physical conditions are required for nanotube formation from bilayer vesicles: (i) the bilayer must be bonded to a spot on a rigid surface, and (ii) there must be a reservoir of excess bilayer surface, beyond that sufficient to enclose the vesicle volume as a sphere. These two conditions are easily attained and manipulated externally. First, vesicles after preparation (*6*) are slightly dehydrated by increasing the osmotic strength of the aqueous suspension. After aspiration into a micropipette, the excess surface of the vesicle is drawn into a projection inside the pipette (Fig. 1A), which

E. Evans and A. Leung, Departments of Physics and Pathology, University of British Columbia, Vancouver, British Columbia, Canada V6T 1W5.
H. Bowman and D. Tirrell, Polymer Science and Engineering Department, University of Massachusetts, Amherst, MA 01003, USA.
D. Needham, Department of Mechanical Engineering and Materials Science, Duke University, Durham, NC 27708, USA.

933